Inner Retinal Oxygen Delivery and Metabolism Under Normoxia and Hypoxia in Rat

Justin Wanek, Pang-yu Teng, Norman P. Blair, and Mahnaz Shahidi

Department of Ophthalmology and Visual Sciences, University of Illinois at Chicago, Chicago, Illinois

Correspondence: Mahnaz Shahidi, Department of Ophthalmology and Visual Sciences, University of Illinois at Chicago, 1855 West Taylor Street, Chicago, IL 60612; mahnshah@uic.edu.

Submitted: February 18, 2013
Accepted: June 21, 2013

Citation: Wanek J, Teng P-Y, Blair NP, Shahidi M. Inner retinal oxygen delivery and metabolism under normoxia and hypoxia in rat. *Invest Ophthalmol Vis Sci*. 2013;54:5012–5019. DOI: 10.1167/iovs.13-11887

Purpose. Retinal hypoxia is a common pathological condition usually caused by ischemia that may result in alterations in oxidative energy metabolism. We report measurements of oxygen delivery by the retinal circulation (DO_{2_IR}) and inner retinal oxygen metabolism (MO_{2_IR}) under systemic normoxia and hypoxia in rat.

Methods. Rats were ventilated with fractions of inspired oxygen (FiO_2) to induce either normoxia ($n = 10$), moderate hypoxia ($n = 14$), or severe hypoxia ($n = 10$). Oxygen tension was measured in retinal vessels using phosphorescence lifetime imaging and converted to arterial (O_{2A}) and venous (O_{2V}) oxygen contents. Total retinal blood flow (F) was assessed by red-free and fluorescent microsphere imaging. DO_{2_IR} and MO_{2_IR} were calculated as the products of F and O_{2A}, and F and the arteriovenous oxygen content difference (O_{2A-V}), respectively.

Results. Measurements of O_{2A}, O_{2V}, and O_{2A-V} were significantly reduced with decreased FiO_2 ($P < 0.001$). In response to reduced oxygen availability, F increased under moderate hypoxia ($P < 0.001$) but did not increase further under severe hypoxia ($P = 0.5$). DO_{2_IR} was similar under normoxia and moderate hypoxia ($P = 0.7$), but significantly lower under severe hypoxia ($P < 0.001$). Likewise, MO_{2_IR} under normoxia and moderate hypoxia was similar ($P = 0.1$), but significantly reduced under severe hypoxia ($P \leq 0.02$).

Conclusions. DO_{2_IR} and MO_{2_IR} were maintained during moderate hypoxia, but reduced under severe hypoxia, indicating blood flow compensation became insufficient for the reduced oxygen availability. Future studies may aid our understanding of retinal metabolic function in ischemic conditions.

Keywords: retina, delivery, metabolism, oxygen, hypoxia

The retina requires a continuous and well-regulated supply of oxygen from the retinal and choroidal circulations to meet its high metabolic demand. Impaired oxygen delivery by the retinal circulation can adversely affect oxygen metabolism and lead to loss of visual function. In fact, abnormalities in retinal oxygenation are believed to contribute to the development of several eye diseases, including glaucoma, diabetic retinopathy, retinal vascular occlusion, and retinopathy of prematurity.[1–4] Therefore, evaluation of the retinal circulation's capacity to meet the oxygen demand of the retinal tissue under physiological and pathological conditions is important.

Oxygen delivery by the retinal circulation (DO_{2_IR}) has been reported in limited studies of newborn animals using combined measurements of retinal blood flow by a radioactive microsphere technique and arterial oxygen content by sampling of arterial blood.[5,6] More commonly, retinal blood flow, an indicator of DO_{2_IR}, has been measured in humans and animals using various techniques, such as Doppler velocimetry,[7–11] Doppler optical coherence tomography (OCT),[12–17] laser speckle,[18,19] microsphere impaction,[20,21] cell labeling,[22–24] and particle tracking.[25,26] However, because DO_{2_IR} is the product of retinal blood flow and arterial blood oxygen content, quantitative measurement of blood flow alone provides only partial information about oxygen delivery to the retina.

Inner retinal oxygen metabolism (MO_{2_IR}) has been previously measured locally in animals using oxygen-sensitive microelectrodes,[27] although three-dimensional oxygen gradients from the retinal microvasculature may have influenced the measurements. To circumvent this problem, MO_{2_IR} has been estimated under experimental conditions of retinal vascular occlusion and 100% oxygen inspiration.[28–30] Alternatively, MO_{2_IR} has been determined globally based on Fick's principle, by directly sampling the oxygen content of arterial and venous blood and measuring blood flow with labeled microspheres,[31,32] as well as using phosphorescence lifetime and fluorescent microsphere imaging techniques.[33] In humans, MO_{2_IR} has been derived by oximetry combined with measurements of blood flow using the laser Doppler technique[34,35] or mean circulation time using fluorescein angiography.[36]

Retinal hypoxia is a common pathological condition usually caused by ischemia[28,37] that occurs in several major retinal diseases and may lead to derangements in oxidative energy metabolism. Despite an abundance of studies that describe the response of retinal blood flow to hypoxia,[5,38–42] there are limited data on DO_{2_IR} and MO_{2_IR} under conditions of reduced oxygen availability.[5,36] The purpose of this study was to report measurements of DO_{2_IR} and MO_{2_IR} under normoxia and systemic hypoxia in rats using combined oxygen tension and blood flow imaging.

METHODS

Animals

Thirty-four Long Evans pigmented rats (weight: 390 ± 72 g, age: 12 ± 3 weeks, mean ± SD) were used in the study. The rats were treated in compliance with the ARVO Statement for the Use of Animals in Ophthalmic and Vision Research. The rats were anesthetized with intraperitoneal injections of ketamine (100 mg/kg) and xylazine (5 mg/kg). Additional injections of ketamine (20 mg/kg) and xylazine (1 mg/kg) were given to maintain anesthesia as required. Rats were mechanically ventilated with three fractions of inspired oxygen (FiO_2), either room air (21% oxygen, normoxia), 15% oxygen (moderate hypoxia), or 10% oxygen (severe hypoxia), with the use of an endotracheal tube connected to a small animal ventilator (Harvard Apparatus, Inc., South Natick, MA). Ventilation with 10% O_2 was selected based on a previously published study,[43] which indicated that this oxygen level produced a maximum or near maximum hypoxic challenge, as evidenced by a significant increase in the retinal oxygen extraction fraction and impairment in the systemic physiological condition. Ventilation with 15% O_2 was selected because it represented an intermediate hypoxic challenge between severe hypoxia and normoxia. Rats were ventilated with reduced FiO_2 gas mixtures 15 minutes before and continuously during imaging for a duration of 1 to 2 hours. To monitor the animal's physiological condition, the femoral artery was cannulated and a catheter was attached to draw blood and connect a pressure transducer. Systemic arterial oxygen tension (P_aO_2), carbon dioxide tension (P_aCO_2), and pH were measured with a blood gas analyzer (Radiometer, Westlake, OH), 5 to 10 minutes after initiation of ventilation. Ventilation parameters, including the respiratory rate and minute volume, were adjusted until the P_aCO_2 was within the normocapnic range.[44] Hemoglobin concentration (HgB) was also measured with a hematology system (Siemens, Tarrytown, NY) from arterial blood. Blood pressure (BP) and heart rate (HR) were monitored continuously with a data acquisition system (Biopac Systems, Goleta, CA) linked to the pressure transducer.

Before imaging, the rat was placed in an animal holder with a copper tubing water heater, which maintained the body temperature at 37°C. The pupils were dilated with 2.5% phenylephrine and 1% tropicamide. A glass cover slip with 1% hydroxypropyl methylcellulose was applied to the cornea to eliminate its refractive power and prevent dehydration. For retinal vascular oxygen tension (PO_2) imaging, an oxygen-sensitive molecular probe, Pd-porphine (Frontier Scientific, Logan, UT), was dissolved (12 mg/mL) in BSA solution (60 mg/mL) and administered through the femoral arterial catheter (20 mg/kg). For retinal blood velocity imaging, 2-μm polystyrene fluorescent microspheres (Invitrogen, Grand Island, NY) were injected through the catheter. Typically, three to four injections of the microspheres were given and each injection was approximately 0.3 mL (10^5 microspheres/mL). One eye of each rat was imaged and data were obtained in 10, 14, and 10 rats under normoxia, moderate hypoxia, and severe hypoxia, respectively.

Retinal Vascular PO_2 Imaging

Retinal vascular PO_2 was measured using our established optical section phosphorescence lifetime imaging system.[45,46] A laser line was projected on the retina after intravenous injection of the Pd-porphine probe and an optical section phosphorescence image was acquired with an intensified charge-coupled device camera. Due to the angle between the excitation laser and imaging path, phosphorescence emissions from the retinal vessels were depth-resolved from the underlying choroid. Phosphorescence lifetimes in the retinal vessels were determined using a frequency-domain approach and converted to PO_2 measurements using the Stern-Volmer equation.[47,48] PO_2 was measured in all major retinal arteries (PO_{2A}) and retinal veins (PO_{2V}), at locations within three optic disc diameters (~600 μm) from the edge of the optic nerve head. Three repeated PO_2 measurements were averaged per blood vessel.

Blood Flow Imaging

Our previously described prototype blood flow imaging system[33] was used for red-free and fluorescent microsphere imaging to assess venous blood vessel diameter and velocity, respectively. A slit lamp biomicroscope with standard light illumination (Carl Zeiss, Oberkochen, Germany) was equipped with a green filter (540 ± 5 nm; Edmund Optics, Barrington, NJ) for red-free retinal imaging, and a 488-nm diode laser (excitation; Melles Griot, Carlsbad, CA), coupled with an emission filter (560 ± 60 nm; Spectrotech, Inc., Saugus, MA) for fluorescent microsphere imaging. Images were captured with a high-speed electron multiplier charge coupled device camera (QImaging, Surrey, Canada). Red-free retinal images were obtained using the full resolution of the camera (1002 × 1004 pixels). For fluorescent images, the camera sensor was binned to maximize the frame rate to 108 Hz, allowing the motion of the microspheres to be resolved in time, but with lower spatial resolution (248 × 250 pixels). Multiple image sequences, each 5 seconds in duration, were recorded over several minutes.

Venous diameter (D) was measured from red-free images over a fixed vessel length (200 μm) that spanned between approximately 300 and 500 μm from the center of the optic disk. Diameter measurements were obtained based on the average full width at half maximum of 12 intensity profiles perpendicular to the blood vessel axis. Venous blood velocity (V) was measured by manually tracking displacements of the microspheres over time, following our previously reported methodology.[33] Typically, three to five image sequences were analyzed to derive V, which was determined by averaging 27 ± 8 microsphere velocity measurements in each vein. The number of velocity measurements was contingent on the number of microspheres that could be visualized in the image sequences. Blood flow in each major vein was calculated from V and D measurements ($V^*\pi^*D^2/4$) and summed over all veins to provide a measure of the total blood flow in the retinal circulation (F). Blood flow was measured in veins because they are less affected by pulsation and have larger diameters as compared with arteries. Measurements of F were obtained approximately 15 minutes following PO_2 imaging, while the physiological state of the animals was relatively stable, as indicated by the continuous monitoring of BP, HR, and the use of constant ventilation parameters.

Oxygen Delivery and Metabolism

The O_2 content of blood was calculated for each major retinal artery and vein as the sum of oxygen bound to hemoglobin and dissolved in blood[49]: O_2 content $= SO_2{}^*C^*HgB + PO_2{}^*k$, where SO_2 is the oxygen saturation, C is maximum oxygen-carrying capacity of hemoglobin (1.39 mL O_2/g),[44] HgB is the measured hemoglobin concentration, PO_2 is the measured vascular oxygen tension, and k is the oxygen solubility in blood (0.003 mL O_2/dL·mm Hg).[50] SO_2 was calculated from the hemoglobin dissociation curve in rat[51] by using the measured PO_2 and arterial blood pH values. Last, in each animal, O_{2A} and

Table 1. Systemic Physiological Parameters (Mean ± SD) Under Normoxia and Graded Levels of Hypoxia

Systemic Physiologic Parameters	Normoxia, $n = 10$	Moderate Hypoxia, $n = 14$	Severe Hypoxia, $n = 10$	P Value
Arterial PO_2, mm Hg	91 ± 9	46 ± 6	31 ± 2	<0.001
Arterial PCO_2, mm Hg	42 ± 3	34 ± 5	39 ± 4	0.001
pH	7.36 ± 0.04	7.40 ± 0.03	7.39 ± 0.05	0.02
BP, mm Hg	101 ± 18	84 ± 17	68 ± 23	0.003
HR, beats/min	224 ± 35	225 ± 31	239 ± 27	0.5
HgB, g/dL	14.2 ± 0.8	14.2 ± 1.0	13.8 ± 0.6	0.5

P values derived by ANOVA are reported.

O_{2V} were determined by averaging the O_2 content of all major retinal arteries and veins, respectively.

DO_{2_IR} was determined from the product of F and O_{2A} measurements according to the following equation:

$$DO_{2\_IR} = F \cdot O_{2A} \quad (1)$$

MO_{2_IR} was calculated from measurements of F and the arteriovenous oxygen content difference (O_{2A-V}), using Fick's principle[52]:

$$MO_{2\_IR} = F(O_{2A} - O_{2V}) \quad (2)$$

Data Analysis

Measurements obtained under normoxia, moderate hypoxia, and severe hypoxia were compared using one-way ANOVA. Linear regression analysis was also performed, demonstrating that PO_{2A}, PO_{2V}, O_{2A}, O_{2V}, V, F, DO_{2_IR}, and MO_{2_IR} were significantly related to BP ($P < 0.004$; $n = 34$), while D and O_{2A-V}, were not ($P \geq 0.2$). Therefore, to adjust for this source of variability, BP was used as a covariate in a one-way analysis of covariance (ANCOVA). Post hoc analyses using Tukey's method were performed to determine statistically significant pairwise differences. All statistical analyses were performed using Systat (Systat Software, Inc., Chicago, IL) and SAS software (SAS Institute, Inc., Cary, NC). Statistical significance was accepted at P less than 0.05.

Results

The systemic physiological status of the rats is summarized according to FiO_2 condition in Table 1. As expected, P_aO_2 was significantly lower under decreased FiO_2 ($P < 0.001$). P_aCO_2 was also significantly different under FiO_2 conditions ($P = 0.001$), but all values were close to or within the normal range of 35 to 45 mm Hg. Similarly, systemic blood pH differed significantly among FiO_2 conditions ($P = 0.02$), although all values were within the normal range of 7.35 to 7.45. No significant changes in HR and HgB were observed with decreased FiO_2 ($P \geq 0.5$). However, BP was significantly reduced with decreased FiO_2 ($P = 0.003$).

Examples of selected cross-sectional vascular PO_2 maps in three rats under different FiO_2 conditions, overlaid on the corresponding red-free retinal images, are shown in Figure 1. Each PO_2 map depicts measurements in major retinal arteries and veins, demonstrating decreased PO_{2A} and PO_{2V} with lower FiO_2. PO_2 was measured in all major retinal arteries and veins of each rat in a similar manner and averaged. Mean values of PO_{2A}, PO_{2V}, O_{2A}, O_{2V}, and O_{2A-V} compiled from measurements in all rats are summarized according to FiO_2 condition in Table 2. All parameters were significantly different among FiO_2 conditions, with and without adjustment for BP ($P < 0.001$). O_{2A} was significantly reduced with each decreased level of FiO_2 ($P < 0.001$), whereas O_{2V} was similar under moderate hypoxia and normoxia ($P = 0.09$), and significantly reduced under severe hypoxia ($P \leq 0.01$). O_{2A-V} was significantly reduced under moderate hypoxia as compared with normoxia ($P < 0.001$), but not statistically different between severe and moderate hypoxia ($P = 0.2$).

An example of a red-free retinal image obtained in one rat under normoxia, displaying major retinal arteries and veins, is shown in Figure 2. Measurements of D, V, and blood flow were obtained in each vein, and the average D and V and the summed total retinal blood flow (F) were calculated. Mean values of D, V, and F compiled from measurements in all rats are summarized according to FiO_2 condition in Table 3. Measurements of D were similar ($P = 0.5$), whereas measurements of V and F were significantly different among FiO_2 conditions, with and without adjustment for BP ($P \leq 0.03$). V was significantly higher under moderate hypoxia as compared with normoxia ($P = 0.003$). F was significantly higher under both moderate and severe hypoxia as compared with normoxia ($P \leq 0.03$), but not statistically different between moderate and severe hypoxia ($P = 0.5$).

Mean values of DO_{2_IR} and MO_{2_IR} according to FiO_2 condition are shown in Figure 3A. DO_{2_IR} and MO_{2_IR} were significantly different among FiO_2 conditions, with and without adjustment for BP ($P \leq 0.002$). There was a significant effect of BP on DO_{2_IR} ($P < 0.001$), but not on MO_{2_IR} ($P = 0.3$). DO_{2_IR} under normoxia (941 ± 231 nL O_2/min) and moderate hypoxia (781 ± 186 nL O_2/min) were similar ($P = 0.7$). Under severe hypoxia, DO_{2_IR} (313 ± 189 nL O_2/min) was significantly lower than under normoxia and moderate hypoxia ($P < 0.001$). Likewise, MO_{2_IR} under normoxia (516 ± 175 nL O_2/min) and moderate hypoxia (377 ± 125 nL O_2/min) were similar ($P = 0.1$). Under severe hypoxia, MO_{2_IR} (182 ± 115 nL O_2/min) was significantly lower than under normoxia and moderate hypoxia ($P \leq 0.02$).

Following Equations 1 and 2, the determinants of DO_{2_IR} and MO_{2_IR} are plotted according to FiO_2 condition in Figures 3B, 3C, respectively. Under moderate hypoxia, DO_{2_IR} and MO_{2_IR} approximated normoxic levels because the reduction in O_{2A} and O_{2A-V}, respectively, was compensated by the increase in F. Under severe hypoxia, DO_{2_IR} was significantly reduced as compared with moderate hypoxia, owing to a further reduction in O_{2A} without an additional compensatory increase in F, presumably due to maximized blood flow compensation. MO_{2_IR} was also significantly reduced under severe hypoxia as compared with moderate hypoxia due to the combined trends of F and O_{2A-V}, even though no significant changes were found in these two parameters individually.

Discussion

Assessment of inner retinal oxygen delivery and metabolism is important for evaluating alterations in retinal metabolic function under hypoxic conditions. In the present study, measurements of DO_{2_IR} and MO_{2_IR} were reported for the first

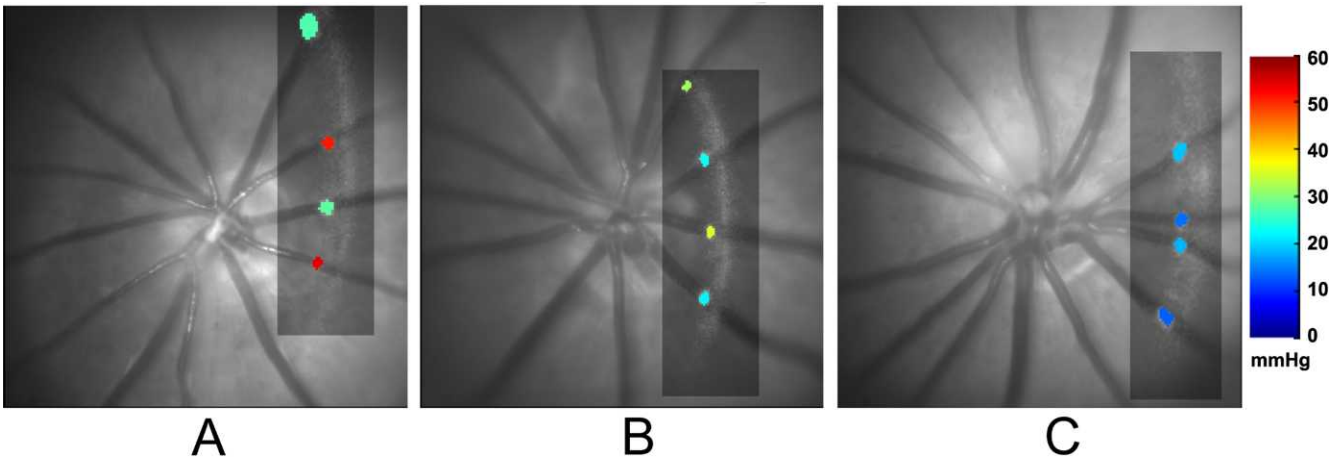

Figure 1. Examples of selected cross-sectional vascular PO_2 maps (*rectangles*) overlaid on red-free retinal images in three rats under (**A**) normoxia, (**B**) moderate hypoxia, and (**C**) severe hypoxia. PO_2 values are depicted in two arteries and two veins. *Color bar* shows PO_2 values in mm Hg.

time in rats and a significant reduction in these parameters was established in response to severe systemic hypoxia.

Hypoxia was induced in rats with controlled ventilation of gases with variable oxygen content. The P_aCO_2 and pH levels were significantly altered, but remained close to their normal ranges due to controlled ventilation parameters. Decreased FiO_2 also resulted in reduced levels of P_aO_2 and BP, consistent with previously published studies in hypoxic animals.[38,53,54] ANCOVA was used to differentiate the effects of FiO_2 and BP, assuming a linear relationship between the measured parameters and the covariate (BP). Although this assumption is not entirely valid, particularly in the presence of autoregulation, highly significant linear regressions of the parameters with BP were determined. Accordingly, using BP as a covariate in ANCOVA allowed elimination of a substantial component of the variability so as to better isolate the effect of FiO_2.

In the current study, measurements obtained under normoxia corresponded with previously published data. Mean PO_{2A} measurements (44 mm Hg) were in general agreement with previously reported values obtained with microelectrodes near the surface of retinal arteries in rats (32 mm Hg),[55] pigs (37 mm Hg),[56] miniature pigs (47 mm Hg),[57] and cats (56 mm Hg).[58] Mean PO_{2V} measurements (26 mm Hg) were also comparable to measurements recorded near retinal veins in rats (19 mm Hg).[55] Mean D measurements (51 μm) were similar to values obtained by in vivo fundus imaging (45 μm)[59] and a corrosion cast technique (53 μm).[60] Similarly, mean V measurements (11.8 mm/s) were in general agreement with previously reported measurements using labeled red blood cells (15.5 and 17.4 mm/s),[24,22] and smaller than a value obtained from microsphere tracking (34.9 mm/s).[25] Although the accuracy of our V measurements may have been limited due to the distribution of velocities that occur with laminar flow, by averaging velocities of multiple microspheres in each blood vessel, this effect was minimized. Mean F measurements (7.9 μL/min) were also similar to values reported using Doppler OCT (6.4 μL/min)[15] and a fluorescent microsphere impaction technique (11.6 μL/min).[61]

To compare DO_{2_IR} and MO_{2_IR} measurements with other published studies, these values were converted to per-unit mass, assuming a retinal mass of 16 mg in rat[62,63] and an inner retinal volume of 50%. DO_{2_IR} was estimated to be 11.8 mLO_2/min*100 g, higher than 5.6 mL O_2/min*100 g reported in newborn lambs.[5] MO_{2_IR} was calculated to be 6.5 mL O_2/min*100 g, slightly higher than values reported in pigs (4.6 and 3.8 mL O_2/min*100 g),[31,32] cats (3.7 mL O_2/min*100 g),[28] and rats (2.7 mL O_2/min*100 g),[30] and lower than whole retinal consumption values determined in humans (9.7 and 8.3 mL O_2/100 mL tissue*100 g).[64,65] These differences may be attributed to the assumed mass and volume of the inner retinal tissue, as well as dissimilarities in methodologies, species, or ages. Another factor that may have affected our estimation of MO_{2_IR} was calculation of O_{2V} from the oxygen dissociation curve using the measured arterial blood pH. Because blood pH tends to be lower in veins as compared with arteries,[66] the actual O_{2V} was probably lower due to a right shift of the oxygen dissociation curve. Therefore, the actual MO_{2_IR} was likely slightly higher than the reported value in the current study.

In response to moderate systemic hypoxia and the consequent reduction in retinal vascular PO_2, F increased significantly due to blood flow compensation for the reduced oxygen availability. This finding is consistent with previously reported retinal blood flow increases in humans,[42] monkeys,[38] cats,[41,67] and newborn lambs[5] during acute systemic hypoxia. The increase in F was predominately due to an increase in V, as

Table 2. Retinal PO_{2A}, PO_{2v}, O_{2A}, O_{2v}, and O_{2A-V} of Rats (Mean ± SD) Under Normoxia and Graded Levels of Hypoxia

Retinal Oxygenation Parameters	Normoxia, $n = 10$	Moderate Hypoxia, $n = 14$	Severe Hypoxia, $n = 10$	ANOVA *P* Value	ANCOVA *P* Value	
				FiO_2	FiO_2	BP
PO_{2A}, mm Hg	44 ± 4	29 ± 4	21 ± 4	<0.001	<0.001	0.7
PO_{2v}, mm Hg	26 ± 3	20 ± 3	12 ± 6	<0.001	<0.001	0.001
O_{2A}, mL O_2/dL	11.9 ± 1.4	7.3 ± 1.7	4.1 ± 1.7	<0.001	<0.001	0.5
O_{2v}, mL O_2/dL	5.4 ± 1.3	3.7 ± 1.2	1.5 ± 1.5	<0.001	<0.001	0.006
O_{2A-V}, mL O_2/dL	6.5 ± 1.5	3.6 ± 1.5	2.6 ± 1.2	<0.001	NA	NA

P values derived by ANOVA and ANCOVA with effects of FiO_2 and BP are reported.

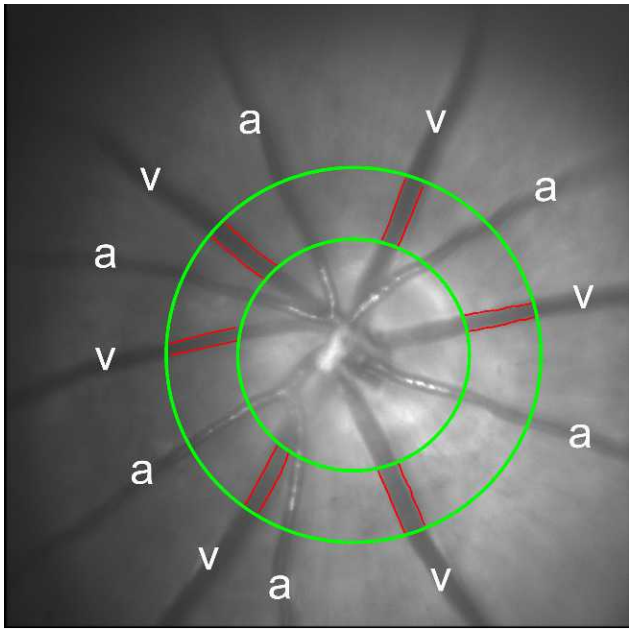

FIGURE 2. An example of a red-free retinal image displaying six major retinal arteries (a) and veins (v) in a rat under normoxia. The outlined edges of the retinal veins (*red lines*) were identified from multiple-diameter measurements over a fixed vessel span at a defined distance from the center of the optic nerve head, as delineated by *green circles*.

a significant change in D was not detected. In accord with our findings, blood velocity has been previously reported to increase under hypoxia,[42,67,68] presumably due to an overall reduction in flow resistance resulting from vasodilation in the retinal microvascular network. Although previous studies have reported dilation of major retinal vessels in response to hypoxia in cats,[67] monkeys,[38] and humans,[69] the relatively large interanimal variability of D likely precluded detection of a statistically significant change in the current study. Under severe hypoxia, F did not increase further as compared with moderate hypoxia, suggesting blood flow compensation was near or at its full capacity.

Alterations in DO_{2_IR} under systemic hypoxia resulted from the opposing effects of the reduced oxygen content of blood and the compensatory increase in blood flow. Under moderate hypoxia, DO_{2_IR} remained relatively stable because the increase in blood flow counteracted the reduction in oxygen availability. This finding is consistent with the previously reported constant DO_{2_IR} values in lambs[5] and relatively unchanged inner retinal tissue PO_2 in cats during acute hypoxia.[70] Under severe hypoxia, the significant decrease in DO_{2_IR} was attributed to a further reduction of available oxygen, without an increase in blood flow, suggesting maximized blood flow compensation capacity under this extreme level of hypoxia.

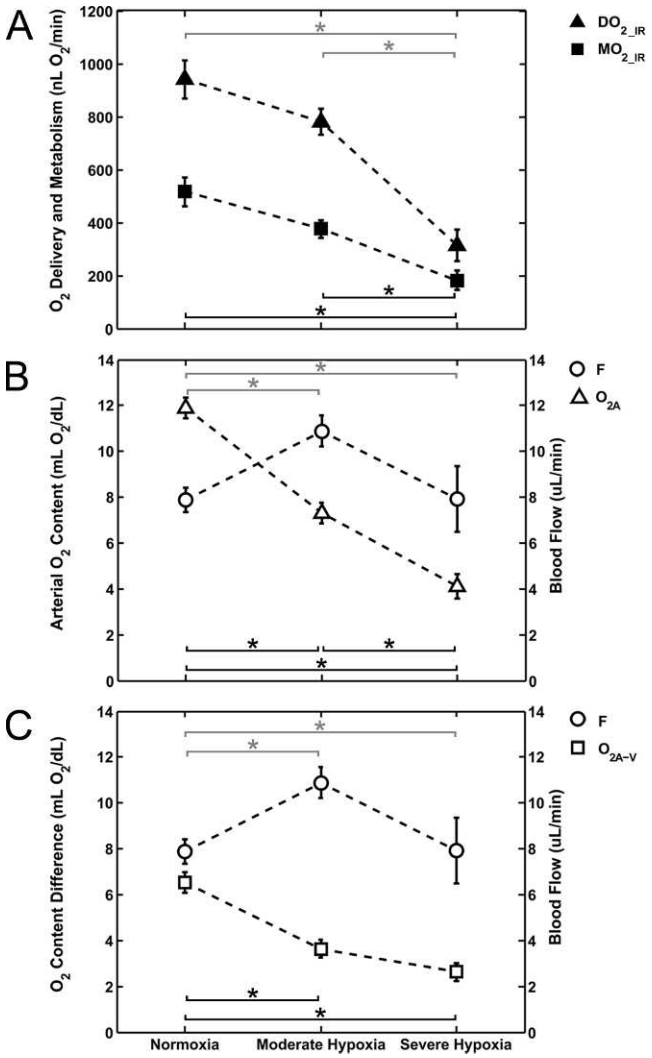

FIGURE 3. (**A**) Mean values of DO_{2_IR} and MO_{2_IR} plotted under normoxia and graded levels of hypoxia. (**B**) The determinants of DO_{2_IR}: F and O_{2A}. (**C**) The determinants of MO_{2_IR}: F and O_{2A-V}. *Error bars* represent the SEM. *Black asterisks* (MO_{2_IR}, O_{2A}, O_{2A-V}) and *gray asterisks* (DO_{2_IR}, F) indicate statistically significant pairwise differences ($P < 0.05$) between FiO_2 conditions based on post hoc analysis.

In the current study, MO_{2_IR} measurements were reported for the first time under hypoxia. Under moderate hypoxia, MO_{2_IR} remained relatively unchanged as compared with normoxia, because DO_{2_IR} did not decline significantly. This finding is in agreement with previously reported steady levels of cerebral oxygen metabolism in rats during moderate levels of hypoxia.[71] However, under severe hypoxia, MO_{2_IR} was significantly reduced due to a considerable decrease in DO_{2_IR}. In fact, a reduction in MO_{2_IR} was inevitable because DO_{2_IR}

TABLE 3. Retinal Venous D, V, and F of Rats (Mean ± SD) Under Normoxia and Graded Levels of Hypoxia

Blood Flow Parameters	Normoxia, $n = 10$	Moderate Hypoxia, $n = 14$	Severe Hypoxia, $n = 10$	ANOVA *P* Value	ANCOVA *P* Value	
				FiO_2	FiO_2	BP
D, μm	51 ± 6	54 ± 6	53 ± 6	0.5	NA	NA
V, mm/s	11.8 ± 2.8	14.3 ± 2.0	9.7 ± 5.2	0.01	0.002	<0.001
F, μL/min	7.9 ± 1.7	10.9 ± 2.5	7.9 ± 4.5	0.03	<0.001	<0.001

P values derived by ANOVA and ANCOVA with effects of FiO_2 and BP are reported.

fell below the normoxic MO_{2_IR} level. Consequently, it was impossible to maintain some energy-requiring processes, which may lead to reduced retinal function and viability.

The severe hypoxic condition investigated in the current study may have initiated metabolic cascades resulting in retinal injury. For example, the expressions of HIF-1α and VEGF in ex vivo retinal tissue of rodents have been shown to increase under short-term hypoxia and ischemia.[72,73] Therefore, it is likely these hypoxic and angiogenic factors would have become elevated in the retinal tissue following severe hypoxia. Furthermore, the observed reduction in MO_{2_IR} under severe hypoxia may have initiated cell apoptosis, as previously demonstrated by elevated levels of proapoptotic markers (Bax and caspase 3) in rats following an ischemic insult.[74,75]

The findings of the current study may have relevance to retinal ischemic conditions associated with hypoxia. For example, in diabetic retinopathy, capillary nonperfusion in localized retinal regions is known to result in reduced DO_{2_IR}, tissue hypoxia, and presumably impaired MO_{2_IR}. The status of the retinal tissue under the severe hypoxic condition in the current study likely bears similarities to ischemic retina in diabetic retinopathy and vascular occlusions. Future studies are needed to investigate the presence and degree of alterations in DO_{2_IR} and MO_{2_IR} in animal models of retinal ischemia.

In summary, combined measurements of inner retinal oxygen delivery and metabolism were reported for the first time in rats under systemic normoxia and graded levels of hypoxia. Blood flow compensation for the reduced oxygen availability maintained inner retinal oxygen delivery and metabolism during moderate hypoxia, but not under severe hypoxia. Future studies with more incremental levels of inspired oxygen are needed to determine the minimum level of oxygen delivery that is required to maintain normal retinal energy metabolism. Because hypoxia is a major consequence of retinal ischemia, findings from such studies will further elucidate the pathophysiology of the retinal ischemic conditions commonly encountered in clinical settings.

Acknowledgments

Supported by the National Eye Institute, Bethesda, Maryland, EY017918 (MS) and EY001792 (UIC); Research to Prevent Blindness, New York, New York, senior scientific investigator award (MS) and an unrestricted departmental award; and University of Illinois at Chicago's Center for Clinical and Translational Science supported by National Center for Advancing Translational Sciences, National Institutes of Health, Bethesda, Maryland, UL1TR000050.

Disclosure: **J. Wanek**, None; **P.-Y. Teng**, None; **N.P. Blair**, None; **M. Shahidi**, P

References

1. Mozaffarieh M, Grieshaber MC, Flammer J. Oxygen and blood flow: players in the pathogenesis of glaucoma. *Mol Vis*. 2008; 14:224–233.
2. Stefansson E. Oxygen and diabetic eye disease. *Graefes Arch Clin Exp Ophthalmol*. 1990;228:120–123.
3. Yoneya S, Saito T, Nishiyama Y, et al. Retinal oxygen saturation levels in patients with central retinal vein occlusion. *Ophthalmology*. 2002;109:1521–1526.
4. Zhang W, Ito Y, Berlin E, Roberts R, Berkowitz BA. Role of hypoxia during normal retinal vessel development and in experimental retinopathy of prematurity. *Invest Ophthalmol Vis Sci*. 2003;44:3119–3123.
5. Milley JR, Rosenberg AA, Jones MD Jr. Retinal and choroidal blood flows in hypoxic and hypercarbic newborn lambs. *Pediatr Res*. 1984;18:410–414.
6. Bottoli I, Beharry K, Modanlou HD, et al. Effect of group B streptococcal meningitis on retinal and choroidal blood flow in newborn pigs. *Invest Ophthalmol Vis Sci*. 1995;36:1231–1239.
7. Feke GT, Tagawa H, Deupree DM, Goger DG, Sebag J, Weiter JJ. Blood flow in the normal human retina. *Invest Ophthalmol Vis Sci*. 1989;30:58–65.
8. Garcia JPS, Garcia PT, Rosen RB. Retinal blood flow in the normal human eye using the canon laser blood flowmeter. *Ophthalmic Res*. 2002;34:295–299.
9. Grunwald JE, Riva CE, Baine J, Brucker AJ. Total retinal volumetric blood-flow rate in diabetic-patients with poor glycemic control. *Invest Ophthalmol Vis Sci*. 1992;33:356–363.
10. Riva CE, Grunwald JE, Sinclair SH, Petrig BL. Blood velocity and volumetric flow-rate in human retinal-vessels. *Invest Ophthalmol Vis Sci*. 1985;26:1124–1132.
11. Riva CE, Feke GT, Eberli B, Benary V. Bidirectional Ldv system for absolute measurement of blood speed in retinal-vessels. *Appl Optics*. 1979;18:2301–2306.
12. Wang Y, Lu A, Gil-Flamer J, Tan O, Izatt JA, Huang D. Measurement of total blood flow in the normal human retina using Doppler Fourier-domain optical coherence tomography. *Br J Ophthalmol*. 2009;93:634–637.
13. Wang YM, Bower BA, Izatt JA, Tan O, Huang D. Retinal blood flow measurement by circumpapillary Fourier domain Doppler optical coherence tomography. *J Biomed Opt*. 2008;13.
14. Werkmeister RM, Dragostinoff N, Pircher M, et al. Bidirectional Doppler Fourier-domain optical coherence tomography for measurement of absolute flow velocities in human retinal vessels. *Opt Lett*. 2008;33:2967–2969.
15. Zhi ZW, Cepurna W, Johnson E, Shen T, Morrison J, Wang RKK. Volumetric and quantitative imaging of retinal blood flow in rats with optical microangiography. *Biomed Opt Express*. 2011;2:579–591.
16. Wang YM, Bower BA, Izatt JA, Tan O, Huang D. In vivo total retinal blood flow measurement by Fourier domain Doppler optical coherence tomography. *J Biomed Opt*. 2007;12: 041215.
17. Leitgeb RA, Schmetterer L, Drexler W, Fercher AF, Zawadzki RJ, Bajraszewski T. Real-time assessment of retinal blood flow with ultrafast acquisition by color Doppler Fourier domain optical coherence tomography. *Opt Express*. 2003;11:3116–3121.
18. Sugiyama T, Araie M, Riva CE, Schmetterer L, Orgul S. Use of laser speckle flowgraphy in ocular blood flow research. *Acta Ophthalmol*. 2010;88:723–729.
19. Nagahara M, Tamaki Y, Tomidokoro A, Araie M. In vivo measurement of blood velocity in human major retinal vessels using the laser speckle method. *Invest Ophthalmol Vis Sci*. 2011;52:87–92.
20. Alm A, Bill A. The oxygen supply to the retina. II. Effects of high intraocular pressure and of increased arterial carbon dioxide tension on uveal and retinal blood flow in cats. A study with radioactively labelled microspheres including flow determinations in brain and some other tissues. *Acta Physiol Scand*. 1972;84:306–319.
21. Alm A, Bill A. Ocular and optic-nerve blood-flow at normal and increased intraocular pressures in monkeys (*Macaca irus*). Study with radioactively labeled microspheres including flow determinations in brain and some other tissues. *Exp Eye Res*. 1973;15:15–29.
22. Nishiwaki H, Ogura Y, Kimura H, Kiryu J, Honda Y. Quantitative evaluation of leukocyte dynamics in retinal microcirculation. *Invest Ophthalmol Vis Sci*. 1995;36:123–130.
23. Le Gargasson JF, Paques M, Guez JE, et al. Scanning laser ophthalmoscope imaging of fluorescein-labelled blood cells. *Graefes Arch Clin Exp Ophthalmol*. 1997;235:56–58.

24. Wajer SD, Taomoto M, McLeod DS, et al. Velocity measurements of normal and sickle red blood cells in the rat retinal and choroidal vasculatures. *Microvasc Res*. 2000;60:281–293.
25. Lorentz K, Zayas-Santiago A, Tummala S, Kang Derwent JJ. Scanning laser ophthalmoscope-particle tracking method to assess blood velocity during hypoxia and hyperoxia. *Adv Exp Med Biol*. 2008;614:253–261.
26. Khoobehi B, Shoelson B, Zhang YZ, Peyman GA. Fluorescent microsphere imaging: a particle-tracking approach to the hemodynamic assessment of the retina and choroid. *Ophthalmic Surg Lasers*. 1997;28:937–947.
27. Cringle SJ, Yu DY, Yu PK, Su EN. Intraretinal oxygen consumption in the rat in vivo. *Invest Ophthalmol Vis Sci*. 2002;43:1922–1927.
28. Alder VA, Ben-Nun J, Cringle SJ. PO2 profiles and oxygen consumption in cat retina with an occluded retinal circulation. *Invest Ophthalmol Vis Sci*. 1990;31:1029–1034.
29. Braun RD, Linsenmeier RA, Goldstick TK. Oxygen consumption in the inner and outer retina of the cat. *Invest Ophthalmol Vis Sci*. 1995;36:542–554.
30. Yu DY, Cringle SJ, Yu PK, Su EN. Intraretinal oxygen distribution and consumption during retinal artery occlusion and graded hyperoxic ventilation in the rat. *Invest Ophthalmol Vis Sci*. 2007;48:2290–2296.
31. Tornquist P, Alm A. Retinal and choroidal contribution to retinal metabolism in vivo. A study in pigs. *Acta Physiol Scand*. 1979;106:351–357.
32. Wang L, Tornquist P, Bill A. Glucose metabolism of the inner retina in pigs in darkness and light. *Acta Physiol Scand*. 1997; 160:71–74.
33. Wanek J, Teng PY, Albers J, Blair NP, Shahidi M. Inner retinal metabolic rate of oxygen by oxygen tension and blood flow imaging in rat. *Biomed Opt Express*. 2011;2:2562–2568.
34. Sebag J, Delori FC, Feke GT, Weiter JJ. Effects of optic atrophy on retinal blood flow and oxygen saturation in humans. *Arch Ophthalmol*. 1989;107:222–226.
35. Siesky B, Harris A, Kagemann L, et al. Ocular blood flow and oxygen delivery to the retina in primary open-angle glaucoma patients: the addition of dorzolamide to timolol monotherapy. *Acta Ophthalmol*. 2010;88:142–149.
36. Hickam JB, Frayser R. Studies of the retinal circulation in man: observations on vessel diameter, arteriovenous oxygen difference, and mean circulation time. *Circulation*. 1966;33:302–316.
37. Pournaras CJ, Tsacopoulos M, Strommer K, Gilodi N, Leuenberger PM. Experimental retinal branch vein occlusion in miniature pigs induces local tissue hypoxia and vasoproliferative microangiopathy. *Ophthalmology*. 1990;97: 1321–1328.
38. Eperon G, Johnson M, David NJ. The effect of arterial PO2 on relative retinal blood flow in monkeys. *Invest Ophthalmol*. 1975;14:342–352.
39. Pournaras C, Tsacopoulos M, Chapuis P. Studies on the role of prostaglandins in the regulation of retinal blood flow. *Exp Eye Res*. 1978;26:687–697.
40. Odden JP, Bratlid D, Hall C, Farstad T, Roll E, Stiris T. Effect of hypoxemia and hypovolemia on retinal and choroidal blood flow in the newborn piglet. *Biol Neonate*. 1993;64:140–150.
41. Ahmed J, Pulfer MK, Linsenmeier RA. Measurement of blood flow through the retinal circulation of the cat during normoxia and hypoxemia using fluorescent microspheres. *Microvasc Res*. 2001;62:143–153.
42. Strenn K, Menapace R, Rainer G, Findl O, Wolzt M, Schmetterer L. Reproducibility and sensitivity of scanning laser Doppler flowmetry during graded changes in PO2. *Br J Ophthalmol*. 1997;81:360–364.
43. Teng PY, Wanek J, Blair NP, Shahidi M. Inner retinal oxygen extraction fraction in rat. *Invest Ophthalmol Vis Sci*. 2013;54: 647–651.
44. West JB. *Pulmonary Physiology and Pathophysiology: An Integrated, Case-Based Approach*. 2nd ed. Philadelphia: Wolters Kluwer Health/Lippincott Williams & Wilkins; 2007: vii, 150.
45. Shahidi M, Shakoor A, Blair NP, Mori M, Shonat RD. A method for chorioretinal oxygen tension measurement. *Curr Eye Res*. 2006;31:357–366.
46. Shahidi M, Wanek J, Blair NP, Mori M. Three-dimensional mapping of chorioretinal vascular oxygen tension in the rat. *Invest Ophthalmol Vis Sci*. 2009;50:820–825.
47. Lakowicz JR, Szmacinski H, Nowaczyk K, Berndt KW, Johnson M. Fluorescence lifetime imaging. *Anal Biochem*. 1992;202: 316–330.
48. Shonat RD, Kight AC. Oxygen tension imaging in the mouse retina. *Ann Biomed Eng*. 2003;31:1084–1096.
49. Shapiro BA, Peruzzi WT, Kozelowski-Templin R. *Clinical Application of Blood Gases*. 5th ed. St. Louis, MO: Mosby; 1994: xviii, 427.
50. Costanzo LS. *Physiology*. 4th ed. Philadelphia: Lippincott Williams & Wilkins; 2007: xii, 334.
51. Cartheuser CF. Standard and pH-affected hemoglobin-O2 binding curves of Sprague-Dawley rats under normal and shifted P50 conditions. *Comp Biochem Physiol Comp Physiol*. 1993;106:775–782.
52. Berne RM, Levy MN. *Physiology*. 2nd ed. St. Louis, MO: Mosby; 1988.
53. Duong TQ. Cerebral blood flow and BOLD fMRI responses to hypoxia in awake and anesthetized rats. *Brain Res*. 2007; 1135:186–194.
54. Johannsson H, Siesjo BK. Cerebral blood flow and oxygen consumption in the rat in hypoxic hypoxia. *Acta Physiol Scand*. 1975;93:269–276.
55. Yu DY, Cringle SJ, Alder V, Su EN. Intraretinal oxygen distribution in the rat with graded systemic hyperoxia and hypercapnia. *Invest Ophthalmol Vis Sci*. 1999;40:2082–2087.
56. Robinson F, Riva CE, Grunwald JE, Petrig BL, Sinclair SH. Retinal blood flow autoregulation in response to an acute increase in blood pressure. *Invest Ophthalmol Vis Sci*. 1986; 27:722–726.
57. Pournaras CJ, Riva CE, Tsacopoulos M, Strommer K. Diffusion of O2 in the retina of anesthetized miniature pigs in normoxia and hyperoxia. *Exp Eye Res*. 1989;49:347–360.
58. Buerk DG, Shonat RD, Riva CE, Cranstoun SD. O2 gradients and countercurrent exchange in the cat vitreous-humor near retinal arterioles and venules. *Microvasc Res*. 1993;45:134–148.
59. Link D, Strohmaier C, Seifert BU, et al. Novel non-contact retina camera for the rat and its application to dynamic retinal vessel analysis. *Biomed Opt Express*. 2011;2:3094–3108.
60. Yamakawa K, Bhutto IA, Lu ZY, Watanabe Y, Amemiya T. Retinal vascular changes in rats with inherited hypercholesterolemia. Corrosion cast demonstration. *Curr Eye Res*. 2001; 22:258–265.
61. Shih YY, Wang L, De La Garza BH, et al. Quantitative retinal and choroidal blood flow during light, dark adaptation and flicker light stimulation in rats using fluorescent microspheres. *Curr Eye Res*. 2013;38:292–298.
62. Brotherton J. Studies on the metabolism of the rat retina with special reference to retinitis pigmentosa. I. Anaerobic glycolysis. *Exp Eye Res*. 1962;1:234–245.
63. Citirik M, Dilsiz N, Batman C, Zilelioglu O. Comparative toxicity of 4 commonly used intravitreal corticosteroids on rat retina. *Can J Ophthalmol*. 2009;44:e3–e8.

Investigative Ophthalmology & Visual Science

64. Anderson B Jr, Saltzman HA. Retinal oxygen utilization measured by hyperbaric blackout. *Arch Ophthalmol*. 1964; 72:792–795.

65. Carlisle R, Lanphier EH, Rahn H. Hyperbaric oxygen and persistence of vision in retinal ischemia. *J Appl Physiol*. 1964; 19:914–918.

66. Oshima T, Karasawa F, Satoh T. Effects of propofol on cerebral blood flow and the metabolic rate of oxygen in humans. *Acta Anaesthesiol Scand*. 2002;46:831–835.

67. Nagaoka T, Sakamoto T, Mori F, Sato E, Yoshida A. The effect of nitric oxide on retinal blood flow during hypoxia in cats. *Invest Ophthalmol Vis Sci*. 2002;43:3037–3044.

68. Sponsel WE, DePaul KL, Zetlan SR. Retinal hemodynamic effects of carbon dioxide, hyperoxia, and mild hypoxia. *Invest Ophthalmol Vis Sci*. 1992;33:1864–1869.

69. Hickam JB, Sieker HO, Frayser R. Studies of retinal circulation and A-V oxygen difference in man. *Trans Am Clin Climatol Assoc*. 1959;71:34–44.

70. Linsenmeier RA, Braun RD. Oxygen distribution and consumption in the cat retina during normoxia and hypoxemia. *J Gen Physiol*. 1992;99:177–197.

71. Hoffman WE, Albrecht RF, Miletich DJ. Cerebrovascular response to hypoxia in young vs aged rats. *Stroke*. 1984;15: 129–133.

72. Kaur C, Sivakumar V, Foulds WS. Early response of neurons and glial cells to hypoxia in the retina. *Invest Ophthalmol Vis Sci*. 2006;47:1126–1141.

73. Ozaki H, Yu AY, Della N, et al. Hypoxia inducible factor-1alpha is increased in ischemic retina: temporal and spatial correlation with VEGF expression. *Invest Ophthalmol Vis Sci*. 1999; 40:182–189.

74. Lam TT, Abler AS, Tso MO. Apoptosis and caspases after ischemia-reperfusion injury in rat retina. *Invest Ophthalmol Vis Sci*. 1999;40:967–975.

75. Kaneda K, Kashii S, Kurosawa T, et al. Apoptotic DNA fragmentation and upregulation of Bax induced by transient ischemia of the rat retina. *Brain Res*. 1999;815:11–20.

Investigative Ophthalmology & Visual Science